Reentrant Condensation of Proteins in Solution Induced by Multivalent Counterions

F. Zhang,[1] M. W. A. Skoda,[1,2] R. M. J. Jacobs,[2] S. Zorn,[1] R. A. Martin,[3] C. M. Martin,[4] G. F. Clark,[4] S. Weggler,[5] A. Hildebrandt,[5] O. Kohlbacher,[6] and F. Schreiber[1,*]

[1]*Institut für Angewandte Physik, Universität Tübingen, Auf der Morgenstelle 10, 72076 Tübingen, Germany*
[2]*CRL, University of Oxford, 12 Mansfield Road, Oxford, OX1 3TA, United Kingdom*
[3]*School of Physical Sciences, Ingram Building, University of Kent, Canterbury, CT2 7NH, United Kingdom*
[4]*SRS, Daresbury, Warrington, Cheshire, WA4 4AD, United Kingdom*
[5]*Zentrum für Bioinformatik Saar, Stuhlsatzenhausweg 85, 66041 Saarbrücken, Germany*
[6]*Zentrum für Bioinformatik Tübingen, Sand 14, 72076 Tübingen, Germany*

(Received 6 February 2008; published 30 September 2008)

Negatively charged globular proteins in solution undergo a condensation upon adding trivalent counterions between two critical concentrations C^* and C^{**}, $C^* < C^{**}$. This reentrant condensation behavior above C^{**} is caused by short-ranged electrostatic interactions between multivalent cations and acidic residues, mechanistically different from the case of DNA. Small-angle x-ray scattering indicates a short-ranged attraction between counterion-bound proteins near C^* and C^{**}. Monte Carlo simulations (under these strong electrostatic coupling conditions) support an effective inversion of charge on surface side chains through binding of the multivalent counterions.

DOI: 10.1103/PhysRevLett.101.148101 PACS numbers: 87.15.km, 61.05.cf, 64.70.D−, 87.15.N−

Effective interactions of biological macromolecules in aqueous solution are generally complex and depend on a number of environmental parameters such as concentration and valence of salt ions, *p*H, and temperature. These complex interactions can give rise to a rich phase diagram. The interactions are also crucial for protein crystallization and many protein aggregation-related physiological diseases [1–3]. Understanding the relationship between the interactions and the resulting phase behavior is thus an important fundamental issue with serious implications for applied science.

The Derjaguin-Landau-Verwey-Overbeek (DLVO) theory has long been used to describe the basic phase behavior and protein interaction in solution [4]. A short-ranged attraction is important for modifying the phase transition in colloidal solutions as well as in protein and DNA solutions [5–13]. The balance between the short-ranged attraction and the long-ranged Coulomb repulsion can lead to equilibrium cluster formation as observed in both protein and colloidal solutions [7,8]. In addition, a long-range attraction is also believed to be important for inducing protein crystallization much more easily than gelation [14–16]. Many studies indicate that the theories based on the mean-field approximation, such as the Gouy-Chapman, Debye-Hückel, and Onsager-Manning theories, fail when the electrostatic coupling becomes strong [17,18].

Reentrant phase transitions are intriguing examples for nontrivial behavior, as found, e.g., in charged colloids [19], DNA, and linear polyelectrolytes [20–25]. Several theories have been proposed to explain the reentrant phenomena induced by multivalent counterions for DNA [21–24]. Among these, charge inversion theory predicts that multivalent counterions condensed on the surface of polyelectrolytes can form a strongly correlated liquid; the charge neutralization and strong correlation among condensed ions account for the charge inversion and the reentrant condensation [23,24]. However, neither theory nor simulation predict a reentrant condensation for a protein solution in the presence of multivalent ions [11,12,18].

In the case of proteins, in contrast to DNA, both positive and negative charges coexist on the surface and in a complex and irregular pattern. Moreover, globular proteins exhibit a different shape (irregular shape versus extended rodlike shape) compared to DNA. It is therefore *a priori* not obvious how proteins behave in the context of the above issues, and most theoretical approaches employed for colloids and DNA are clearly inapplicable to this case [26].

In this Letter, we report for the first time a reentrant condensation behavior in aqueous protein solution induced by addition of multivalent counterions. Based on optical transmission and small-angle x-ray scattering (SAXS) data we deduce the effective protein-protein interactions and construct a phase diagram. We also provide a possible theoretical explanation of the effect that is supported by Monte Carlo simulations of the charge distribution of proteins at different counterion concentrations.

Model globular proteins bovine serum albumin (BSA) (A3059) and ovalbumin (A5503) from chicken egg white were purchased from Sigma-Aldrich and used as received. BSA is negatively charged above its isoelectric point of *p*H 4.6. Yttrium chloride (45,136-3) was purchased from Sigma-Aldrich and lanthanum chloride (AB112424) was purchased from ABCR GmbH, Karlsruhe, Germany. A series of protein solutions with various salt concentrations was prepared and the phase behavior was determined by monitoring the optical transmission. Protein interactions of selected samples were studied by SAXS at beam line

MWP6.2 at the Daresbury synchrotron radiation source, with an accessible q range of 0.008–0.25 $Å^{-1}$. The data collection, calibration, and data fitting followed the procedures described in Ref. [16].

Figure 1(a) displays a photograph of a series of samples showing phase transitions near two critical salt concentrations. At a BSA concentration of 50 mg/mL, phase separation as evidenced by the turbid solution occurs in the range $C^* < [Y^{3+}] < C^{**}$; outside of this region, a homogeneous solution is observed. Fourier-transform infrared spectra for the solutions below C^* and above C^{**} indicate that proteins are still in their native state (data not shown). The transmission intensity of a series of samples at a protein concentration of 20 mg/mL as a function of salt concentration has been measured at 632.8 nm with a photodiode detector [Fig. 1(b)]. The evolution of transmission intensity clearly shows a fairly abrupt phase separation approaching C^* and a subsequent increase of intensity (reentrant condensation) upon further increasing the salt concentration. Over extended periods of time (many hours to days) the aggregates in the turbid solutions precipitate, and hence the exact position of C^{**} becomes less well defined. We have also tested BSA with La^{3+}, and ovalbumin with Y^{3+} and La^{3+}, and observed the reentrant condensation in all cases, in contrast to monovalent salt such as NaCl, where no condensation has been observed.

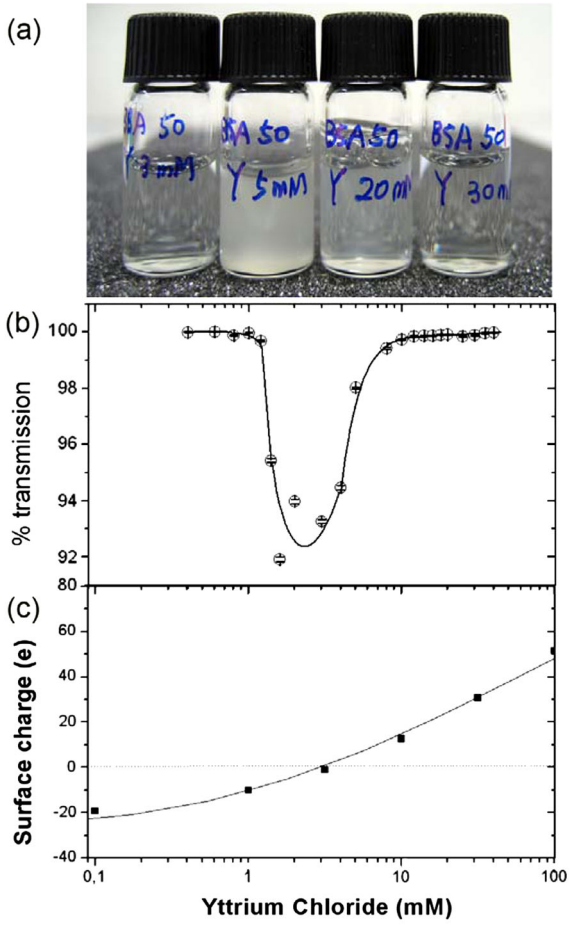

FIG. 1 (color online). (a) Photograph of sample cells showing the reentrant condensation with increasing salt concentration. BSA 50 mg/mL, $C^* \sim 4$ mM $< [Y^{3+}] < C^{**} \sim 25$ mM, gives a phase separated (turbid) solution, outside of this region, it gives a homogeneous solution. (b) Optical transmission as a function of Y^{3+}, BSA 20 mg/mL, $C^* \sim 1.0$ mM, and $C^{**} \sim 11$ mM. (c) Predicted charge of BSA surface residues at specific Y^{3+} concentrations based on a Monte Carlo simulation (see text for details).

Figure 2 shows a phase diagram of BSA solution in the presence of trivalent counterion Y^{3+} as a function of protein and salt concentration. Three regimes are recognized: in regime I with $C < C^*$, one fluid phase exists; in regime II with $C^* < C < C^{**}$, two phases exist; and in regime III with $C > C^{**}$, again one fluid phase exists.

At this point, the reentrant phase transition and the phase diagram are established by the associated macroscopic behavior. In order to investigate the underlying mechanisms, we will now turn to the microscopic interactions.

As a first step, the *effective* protein-protein interaction is investigated by SAXS. The scattering intensity $I(q)$ of monodisperse nonspherical particles can be related to the effective structure factor $\bar{S}(q)$ in an average structure factor approximation and the form factor $P(q)$, by the relation $I(q) = N_p(\Delta\rho)^2 V_P^2 P(q)\bar{S}(q)$, where N_P is the number density of protein in solution, V_P is the volume of a single protein, $\Delta\rho$ is the difference between the electron density of proteins and that of the solvent, the scattering vector $q = (4\pi/\lambda)\sin(2\theta/2)$, and 2θ is the scattering angle. $\bar{S}(q)$ is calculated using a monodisperse structure factor with an effective sphere diameter. In our case, the protein solution is a monodisperse but nonspherical (ellipsoidal) system.

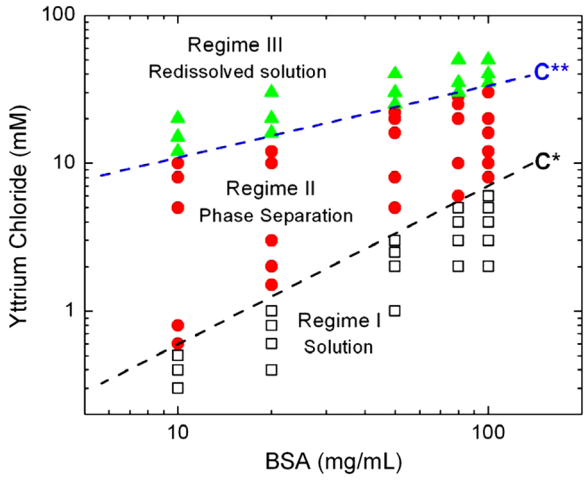

FIG. 2 (color online). Phase diagram of BSA solution as a function of protein and salt concentration. The symbols indicate individual samples in the respective regimes. Note that all data on C^* and C^{**} are taken on the time scale of minutes; for very long times (many hours to days) the solution becomes clear again as the aggregate precipitates.

The effective sphere diameter is calculated by equating the second virial coefficient A_2 of the ellipsoid to a sphere having the same A_2. This effective diameter is then used to calculate $\bar{S}(q)$ [16,27].

Figure 3(a) presents the typical SAXS intensity, $I(q)$, in the vicinity of C^* for a protein concentration of 100 mg/mL. For comparison, the scattering profile of a solution with 20 mM monovalent salt, NaBr, is also shown. With 20 mM NaBr, the scattering intensity shows a strong correlation peak at $q^* = 0.05$ Å^{-1}. The system is characterized by a repulsive interaction, which can be described by DLVO theory [16]. The repulsion originates from the surface charge of proteins. Addition of 3 mM YCl_3 reduces the strength of repulsive potential. Upon further increase to 5 mM, and 6 mM, slightly below and above C^*, respectively, a clear increase of $I(q)$ at low q was observed, indicating the evolution of attractive interactions. A square-well structure factor was used to fit the data [Fig. 3(b)] [27]. The square-well potential is described as

$$U_{\mathrm{SW}}(r) = \begin{cases} a & 0 < r < D \\ -u & D < r < \delta D \\ 0 & \delta D < r, \end{cases}$$

where D is the hard sphere diameter and u and δ are depth and width (in units of the effective diameter) of the attractive well, respectively. At 5 mM, $u \sim 2k_BT$ and $\delta = 1.06$ were obtained. At 6 mM, i.e., slightly above C^*, the solution becomes turbid; the data fitting gives a much higher well depth of $\sim 5.4k_BT$, with a similar well width of $\delta = 1.10$. Above C^{**} [Figs. 3(c) and 3(d)], the interaction is still a short-ranged attraction. However, the strength of the attraction decreases with salt concentration as seen from the decrease of $I(q)$ and $S(q)$ in the low q range. Data fitting gives well depths of 7.5, 6.9, and $3.4k_BT$ for YCl_3 of 40, 50, and 100 mM, respectively. The well widths are

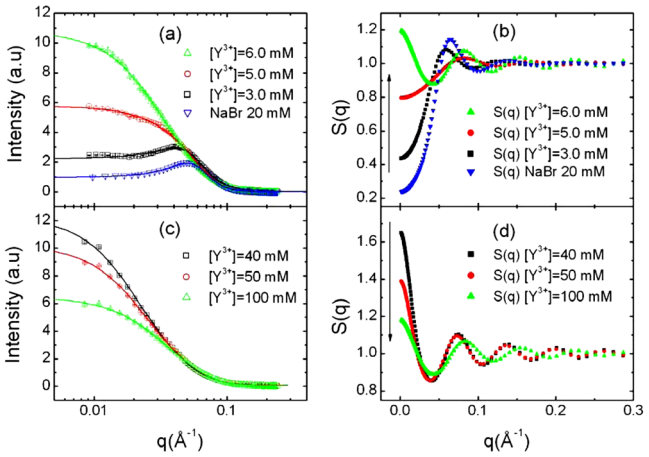

FIG. 3 (color online). Experimental SAXS data with model fitting for protein solutions with Y^{3+} (a) below and around C^* and (c) above C^{**} for BSA 100 mg/mL; (b),(d) show the corresponding structure factor evaluated from data fitting.

1.16, 1.20, and 1.23 (in units of the effective diameter). The SAXS results clearly show that addition of YCl_3 induces a short-ranged attraction between proteins, and the strength (well depth) increases with salt concentration before C^* and decreases after C^{**}. Therefore, we observe phase separation (aggregation) if the attraction is strong enough, and, upon further increase of salt concentration, a gradual reduction of the attraction, leading to redissolution, in good agreement with Fig. 1.

While the optical transmission data and the SAXS results are consistent, they provide information only on the *effective* interactions. In order to shed light on the microscopic mechanisms, we employed a computer simulation. The most obvious influence of the multivalent yttrium ions on BSA is electrostatic. Hence, a theoretical study of the electrostatics of BSA promises to yield insights into the condensation process. Y^{3+} ions interact preferably with solvent-exposed negatively charged side chains (Asp, Glu), thus modulating the surface charge distribution. We have developed a simulation approach, which estimates the likelihood of complexation of the carboxylate groups of Asp and Glu on the BSA surface with Y^{3+} ions. A naïve approach, based on simple electrostatic computations, must be expected to fail since it is well known that mean-field methods fail to account correctly for the strongly correlated multivalent counterions. The fundamental difference in surface charge distribution, size, and shape renders the application of hard sphere models or rodlike models popular for colloids and DNA inappropriate [28]. Hence, we explicitly model the strongly bound counterions to account for a significant part of the correlation, namely, that of bound Y^{3+} with the protein and of multiple yttrium ions bound with one another. Our simulation is inspired by methods used for the prediction of side chain protonation [28]. It performs a Monte Carlo sampling of an approximate partition function for BSA-yttrium complexation. This approach samples from all possible ion arrangements and considers full protein-ion and ion-ion interactions, including counterion rearrangements. For various Y^{3+} concentrations the electrostatic potential at the site of each exposed carboxylate group of BSA was computed with a Poisson-Boltzmann solver [29]. Using an experimental estimate of the association constant of Y^{3+} with a carboxylate group [30], the likelihood of Y^{3+} ions binding to acidic surface side chains has been predicted for varying Y^{3+} concentrations. Since the three-dimensional structure of BSA is not exactly known, the study is based on a homology model based on the very similar human serum albumin (HSA, 76% sequence identity to BSA). The model was built using PRIME (Schrödinger Inc., New York, release 1.6.307) based on the sequence of BSA and the structure of HSA (Protein Data Bank ID 1N5U). Side chain protonation states were predicted using H++ [31]. While the approximations involved will certainly result in some inaccuracies, based on our extensive test [32], we still expect

the qualitative effect of a surface charge inversion to be correctly reproduced. Figure 1(c) shows the resulting surface charge of BSA as a function of Y^{3+} concentration. The surface-exposed side chains of BSA undergo an effective charge inversion over the Y^{3+} concentration range considered in our experiments, which will obviously modulate the electrostatic interactions, both long- and short-ranged.

Combining the experimental and the theoretical results helps to understand the condensation behavior observed. To explain the overall behavior, one must consider three main effects: long-range electrostatic interactions, short-range electrostatic interactions, and entropic contributions. Long-range electrostatic interactions are dominated by the net charge of the proteins and the surrounding counterions. Short-range electrostatic interactions are interactions between well-localized charges (side chains and bound Y^{3+}) on the protein surfaces. Entropic contributions account primarily for hydrophobic effects and the loss of degrees of freedom. BSA condensation is governed by the *sum* of these effects. It is difficult to predict the precise balance of these interactions; however, it seems plausible that long-range electrostatic repulsion is the reason for the prevention of protein condensation at both low and high concentrations (regime I + III). This agrees with the predicted large absolute surface charges at low and high Y^{3+} concentrations seen in Fig. 1(c) and SAXS results in Fig. 3(a). Note that at high salt concentration, the attractive potential with reduced strength from SAXS measurements indicates that it is the balance of short-range attraction and long-range repulsion which leads to the redissolution of precipitates. It is known that this balance can result in equilibrium cluster formation in both protein and colloid solutions [7,8]. The repulsive interactions are compensated by attractive interactions (short-range charge correlations and hydrophobic interactions) at intermediate concentration ranges leading to precipitation of BSA.

In order to fully understand the effect, further theoretical studies are required. Simple theories like DLVO, which are highly valuable in the colloidal context, are not appropriate for our problem because of the complex charge distribution and geometries involved. While other theoretical approaches, in particular, Debye-Hückel and related theories, work well for complex geometries, they fail for large screening charges. For highly charged ions, ion-ion correlations become important and mean-field approaches fail [18]. A full understanding of reentrant BSA condensation in the presence of Y^{3+} will thus require the application of post-DLVO theories. Until such methods are available, a study of the multipole moments of BSA as well as the behavior of the counterion ''cloud'' around the protein might provide insights into the balance of the different interactions.

In summary, we have presented the first experimental observations of reentrant condensation of model globular proteins in solution in the presence of trivalent counterions, which is supported by a Monte Carlo simulation suggesting a surface charge inversion. This observation provides a new way to tune protein interactions in solution.

We acknowledge financial support from the EPSRC.

*Corresponding author.
frank.schreiber@uni-tuebingen.de

[1] S. D. Durbin and G. Feher, Annu. Rev. Phys. Chem. **47**, 171 (1996).
[2] V. J. Anderson and H. N. W. Lekkerkerker, Nature (London) **416**, 811 (2002).
[3] R. Piazza, Curr. Opin. Colloid Interface Sci. **8**, 515 (2004).
[4] A. Tardieu *et al.*, J. Cryst. Growth **196**, 193 (1999).
[5] N. Asherie, A. Lomakin, and G. B. Benedek, Phys. Rev. Lett. **77**, 4832 (1996).
[6] D. Rosenbaum, P. C. Zamora, and C. F. Zukoski, Phys. Rev. Lett. **76**, 150 (1996).
[7] A. Stradner *et al.*, Nature (London) **432**, 492 (2004).
[8] F. Sciortino *et al.*, Phys. Rev. Lett. **93**, 055701 (2004).
[9] X. Qiu *et al.*, Phys. Rev. Lett. **96**, 138101 (2006).
[10] Y. Bai *et al.*, Proc. Natl. Acad. Sci. U.S.A. **102**, 1035 (2005).
[11] P. Linse and V. Lobaskin, Phys. Rev. Lett. **83**, 4208 (1999).
[12] M. Lund and B. Jönsson, Biophys. J. **85**, 2940 (2003).
[13] N. Javid *et al.*, Phys. Rev. Lett. **99**, 028101 (2007).
[14] M. G. Noro, N. Kern, and D. Frenkel, Europhys. Lett. **48**, 332 (1999).
[15] Y. Liu *et al.*, Phys. Rev. Lett. **95**, 118102 (2005).
[16] F. Zhang *et al.*, J. Phys. Chem. B **111**, 251 (2007).
[17] Y. Levin, Rep. Prog. Phys. **65**, 1577 (2002).
[18] A. Y. Grosberg, T. T. Nguyen, and B. I. Shklovskii, Rev. Mod. Phys. **74**, 329 (2002).
[19] *Ordering and Phase Transitions in Charged Colloids*, edited by A. K. Arora and B. V. R. Tata (VCH, New York, 1996), Chap. 6.
[20] V. A. Bloomfield, Curr. Opin. Struct. Biol. **6**, 334 (1996).
[21] M. Olvera de la Cruz *et al.*, J. Chem. Phys. **103**, 5781 (1995).
[22] F. J. Solis and M. Olvera de la Cruz, J. Chem. Phys. **112**, 2030 (2000).
[23] T. T. Nguyen, I. Rouzina, and B. I. Shklovskii, J. Chem. Phys. **112**, 2562 (2000).
[24] B. I. Shklovskii, Phys. Rev. Lett. **82**, 3268 (1999); Phys. Rev. E **60**, 5802 (1999).
[25] J. C. Butler *et al.*, Phys. Rev. Lett. **91**, 028301 (2003).
[26] T. Nicolai and D. Durand, Curr. Opin. Colloid Interface Sci. **12**, 23 (2007).
[27] S. R. Kline, J. Appl. Crystallogr. **39**, 895 (2006).
[28] M. Schaefer, M. Sommer, and M. Karplus, J. Phys. Chem. B **101**, 1663 (1997).
[29] N. A. Baker *et al.*, Proc. Natl. Acad. Sci. U.S.A. **98**, 10 037 (2001).
[30] R. S. Sandhu, Monatsh. Chem. **108**, 51 (1977).
[31] J. C. Gordon *et al.*, Nucleic Acids Res. **33**, W368 (2005).
[32] A. Hildebrandt *et al.* (to be published).